IEEE Access
Multidisciplinary | Rapid Review | Open Access Journal

Received 25 May 2024, accepted 9 June 2024, date of publication 11 June 2024, date of current version 19 June 2024.

Digital Object Identifier 10.1109/ACCESS.2024.3412991

RESEARCH ARTICLE

Artificial Neural Networks-Based Fault Localization in Distributed Generation Integrated Networks Considering Fault Impedance

ARASH MOUSAVI [1], RASHIN MOUSAVI[1], YASHAR MOUSAVI[2], (Member, IEEE), MAHSA TAVASOLI[3], ALIASGHAR ARAB[4], (Member, IEEE), AND AFEF FEKIH[5], (Senior Member, IEEE)

[1]Department of Electrical Engineering and Applied Sciences, Paradise Research Center, Jahrom 74168-13647, Iran
[2]Department of Applied Science, School of Computing, Engineering and Built Environment, Glasgow Caledonian University, G4 0BA Glasgow, U.K.
[3]Department of Applied Science and Technology, North Carolina Agricultural and Technical State University, Greensboro, NC 27411, USA
[4]Department of Electrical and Computer Engineering, Tandon School of Engineering, New York University, New York, NY 11201, USA
[5]Department of Electrical and Computer Engineering, University of Louisiana at Lafayette, Lafayette, LA 70504, USA

Corresponding author: Yashar Mousavi (seyedyashar.mousavi@gcu.ac.uk)

ABSTRACT This paper proposes a fault location and protection method for power distribution system with Distributed generation (DG) resources, considering fault impedance. A multi-layer perceptron (MLP) Artificial Neural Network (ANN)-based approach using the Levenberg-Marquardt algorithm to train the neural network for fault location and identification within distribution networks with DGs is developed. The proposed method emphasizes the incorporation of fault impedance in the analytic process. It also leverages the robust computational capabilities and inherent simplicity of ANNs to accurately detect the fault type and subsequently identify the fault location. Furthermore, it implements a zoning strategy, which partitions the distribution system into multiple independent sections to facilitate a more organized and effective fault management process. Simulation results and conducted analyses confirmed the effectiveness of the proposed approach in localizing faults within the network thereby minimizing downtime during faulty conditions and improving power system's capabilities and reliability. Among the key advantages of the proposed fault detection approach are its ability to adeptly handle the complexities introduced by the wide integration of DGs in distribution networks.

INDEX TERMS Fault location, distribution networks, distributed generation sources, neural networks.

I. INTRODUCTION

Power distribution systems are increasingly prone to faults due to environmental impacts, such as lightning, trees falling onto lines, and infrastructure issues, such as aging and low maintenance, leading to insulation breakdowns, which disrupt power supply continuity and reliability [1], [2], [3], [4]. The primary role of the protection system is to detect faults promptly and isolate the faulty feeder, followed by accurately estimating the fault's location. Accurate fault localization conserves maintenance time, reduces service interruption duration, and enhances reliability indices. However, as electrical power networks, including distribution networks, expand, traditional network management and control methods become inadequate [5], [6]. The faults in distribution networks, often characterized by high impedance, pose challenges in detection and precise localization by protective equipment. Consequently, some sections of the network without faults may be unnecessarily disconnected, resulting in extended downtimes for fault localization [7], [8]. This inefficiency increases the definitive time required for network restoration, calling for

The associate editor coordinating the review of this manuscript and approving it for publication was Fabio Mottola.

more efficient alternative network management and control methods [9], [10], [11].

In the electric power industry's competitive markets and the increased focus on customer satisfaction, ensuring customers' certainty is paramount for consumers and network administrators. Delays in fixing problems can make networks unreliable, costing network companies lower sales and payments for service disruptions [12], [13]. These challenges compound the complexity of tasks for maintenance teams, especially when locating and rectifying faults in inaccessible areas. Consequently, there's a pressing need for innovative solutions that expedite the fault location process while minimizing human intervention and physical constraints [14], [15], [16]. The fault location is a critical aspect of power system protection, directly impacting the reduction of undistributed energy, boosting system profitability, and enhancing customer satisfaction with the power supply [17], [18], [19], [20], [21]. On the other hand, the application of coordinate control within a medium voltage DC grid enhances system resilience and operational efficiency while implementing fault location algorithms, which present intricacies [22], [23], [24], [25], [26], especially in distribution networks that are crucial to power system protection due to their proximity to consumers [27], [28], [29]. This complexity stems from factors such as the extensive and varied sub-branches, discrepancies in cross-sections and phase arrangements in overhead lines and underground cables, and the presence of distribution transformers with diverse nominal capacities across the network. In addition, integrating distributed generation (DG) into modern networks introduces further challenges in fault identification despite research indicating the cost-effectiveness of DG systems over expanding transmission and sub-transmission networks [30], [31], [32], [33]. High impedance faults (HIFs), caused by unintended contact between a bare-energized conductor and a poorly grounded object, pose a particularly concerning issue [34], [35]. In this context, conventional overcurrent devices often fail to detect HIFs due to their restricted fault current flow. Unlike typical faults, HIFs exhibit non-linear voltage-current characteristics influenced by electric arcs and changing surface conditions. Addressing these complex dynamics necessitates a nuanced approach to fault location in distribution networks, underscoring the importance of research and development in advanced fault location methodologies.

Fault location methodologies in power systems fall into three major categories: traditional, observant, and intelligent approaches. Minimizing fault-location method errors within the distribution networks is vital [36]. The improvement mainly relies on having precise system data supported by rapid and reliable communication networks, resilient control systems, and advanced algorithmic thinking for decisions. The conventional method includes instances such as observation—where customers might inform the utility of issues such as fallen cables or the scent of burning wires. The observant approach involves using smart meters or local sensors to alert the system operators through communication

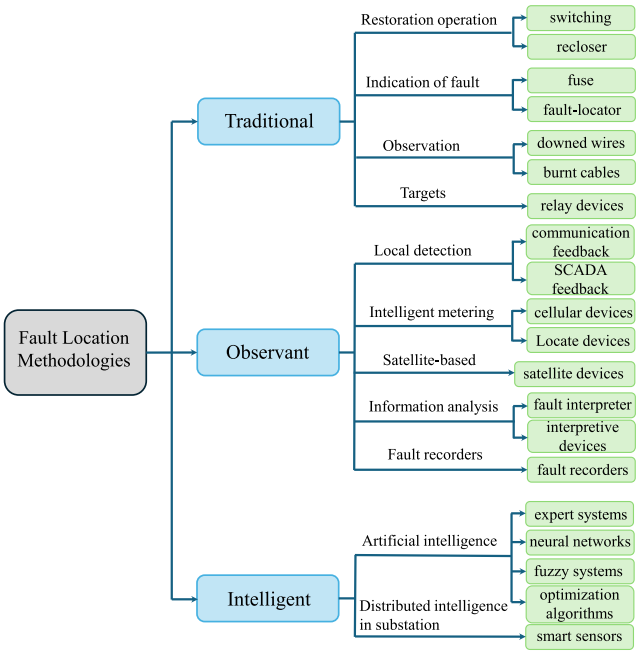

FIGURE 1. Fault location approaches for power distribution systems.

channels. The intelligent approaches [37], [38], [39], on the other hand, utilize advanced sensors or expert systems, including artificial neural networks (ANN) and optimization algorithms, to identify faults [40], [41]. Figure 1 depicts a representation of these approaches [42], [43].

Recent years have witnessed considerable investigations in advancing fault location techniques for distribution networks, particularly focusing on impedance-based methodologies and integrating artificial intelligence to enhance precision and adaptability [44], [45], [46], [47], [48], [49], [50], [51]. These methods primarily utilize fundamental RMS voltage and current measurements at substations to estimate impedance and thereby deduce the fault's distance within the network [52]. Researchers have investigated various approaches that include algorithms to compute fault reactance across feeders and mitigate fault resistance effects alongside direct circuit analysis techniques investigated for unbalanced systems, addressing specific fault types such as line-to-line or single-line-to-ground faults [53], [54], [55]. However, despite their merits, these methods deal with challenges such as iterative error accumulation or the need for extensive data for training and tuning algorithm parameters. The development of effective fault location strategies is further complicated by the inherent characteristics of distribution systems, such as radial topology, the presence of short and heterogeneous lines, and limited instrumentation. Consequently, an effective approach that leverages system knowledge, historical data, and external information is imperative [56], [57]. Recent studies have explored many HIF detection techniques, employing diverse methodologies such as wavelet transforms, pattern recognition, Bayes classifiers, empirical mode decomposition, and multiresolution analysis [58], [59]. While

promising, these methods often rely on extensive parameter sets and face challenges in real-time applications due to the dynamic topology of distribution networks and computational demands. Emerging research suggests innovative detection methods for high- and low-impedance faults, utilizing the Stockwell Transform (ST) without NN support or in conjunction with the Hilbert transform [60], [61], [62], [63]. Although these approaches show notable detection rates, they are critiqued for their limited impedance range and lack of specificity in frequency range analysis. As a consequence, concerns will be rising about their ability to distinguish HIFs from other events with similar harmonic content variations, which highlights the need for continuous refinement and integration of diverse knowledge sources to enhance the accuracy and reliability of fault location in distribution networks, considering the intricate interplay of fault impedance and network dynamics. Due to the complexity of distribution systems and various uncertainty factors that are difficult to address using conventional approaches, knowledge-based techniques are applied for locating faults, where a fast and efficient fault location approach is of utmost importance. In this respect, an investigation of various knowledge-based fault localization methodologies considering fault impedance in DG networks is provided. The methodologies include conventional approaches such as k-nearest neighbors (k-NN) and decision trees (DT), alongside more sophisticated techniques involving optimization algorithms, fuzzy logic, ANN, support vector machines (SVM), and deep neural networks (DNN). Each method is evaluated for its merits and limitations within this specific application, as illustrated in Table 1.

This study develops an ANN-based approach for fault location identification within distribution networks, emphasizing the incorporation of fault impedance in the analytic process. The work primarily inspects the precision of fault localization by analyzing voltage and flow parameters at the commencement of distribution lines. Furthermore, the impact of multiple distributed generation sources is considered, noting their varied installation locales. Recognizing the efficacy of ANNs in addressing complex engineering challenges, such as function estimation and categorization, this research leverages the robust computational capabilities and inherent simplicity of ANNs. These attributes have notably helped the adoption of ANNs in solving intricate problems. This research introduces and examines a protective scheme that adeptly identifies the precise coordinates of faults within distribution networks enriched with distributed generation sources. The methodology proposed herein is distinguished by its accuracy in identifying fault types and locations; it achieves this by carefully examining fault resistance and using the computing power of ANNs.

The remainder of this paper is structured as follows. Section II investigates the fault localization concepts. The proposed fault localization approach is presented in Section III. The performance of the proposed approach is evaluated in Section IV. Section V concludes the paper.

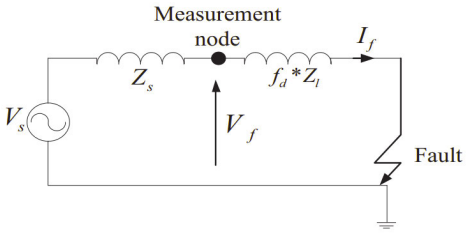

FIGURE 2. Impedance-based method.

II. FAULT LOCALIZATION

The variability of fault impedance in distribution systems introduces considerable complexity to fault location processes, making them more challenging than analogous procedures in generation and transmission systems. Furthermore, the economic implications of equipping low-cost distribution network components with advanced protective mechanisms are unfavorable. Conversely, the implementation of protective systems significantly enhances network reliability by facilitating accurate fault positioning [71]. Traditional algorithms for fault location are predominantly implemented for transmission systems and, consequently, are not directly applicable to radial distribution networks. The algorithms provided for distribution networks are developed with a focus on the classification and modeling of multiple fault locations, predicated on a methodology of progressive approximation. Impedance-based approaches are favored by electric power academic and industrial investigators due to their straightforwardness and cost-effectiveness compared to the traveling wave method. The main idea of the impedance method is to employ the impedance observed from the measurement point to pinpoint faults by taking voltage and current measurements to figure out the impedance. Figure 2 illustrates the impedance-based method using a simple circuit representation. In this model, V_f represents the fault voltage, I_f denotes the fault current, and Z_i is defined as the line impedance per unit length. The variable f_d indicates the fault distance from the measurement node, and V_s and Z_s are the source voltage and source impedance, respectively. Employing Ohm's Law, one can calculate the fault distance from the measurement node as:

$$f_d = \frac{V_f}{I_f \times Z_i}. \tag{1}$$

The developed diagnostic and location framework for faults comprises three phases: signal processing, location, and diagnosis. The algorithm for fault location operates on a repetitive solution-finding approach for equations characterizing the fault under steady-state conditions. It takes into account the current and voltage values at the terminal end of the faulted linear section and considers the interaction effects on the phases. The relationship governing the faulty phase is represented as follows:

$$V_a = D(Z_{ab}I_b = Z_{ac}I_c) + I_f R_f, \tag{2}$$

TABLE 1. Comparison of k-NN, DT, optimization algorithms, fuzzy logic, ANN, SVM, and DNN approaches for fault localization in distributed generation integrated networks considering fault impedance.

Method	Advantages	Disadvantages
k-NN [64]	- Simple implementation; adjusts flexibly to changes. - Does not make assumptions about data distribution.	- Computationally expensive with large datasets. - Sensitive to noisy data and irrelevant features.
DT [65]	- Transparent decision-making process. - Effective with both numerical and categorical data. - No feature scaling needed.	- Susceptible to overfitting. - Biased if some classes are dominant. - Less appropriate for precise fault estimation.
Optimization algorithms [12]	- Capable of exploring diverse solutions globally. - Facilitates feature and parameter optimization.	- Often slow to converge, requiring multiple iterations. - Does not always guarantee optimal solutions.
Fuzzy logic [1]	- Manages uncertainties and interprets relationships with rules. - Tolerates imprecise data, applicable to systems with variable fault impedance.	- Finding the global minimum with fuzzy membership functions is complex. - Membership functions and rules design is intricate. - Requires advanced feature definition and extraction.
ANN [1], [66], [67]	- High accuracy and adaptability for complex environments with distributed generation. - Proficient in noise and high impedance fault handling. - Utilizes fault impedance analysis for enhanced precision. - Effective zoning strategy for fault management.	- Requires large data and computational resources for training. - Model training and updates are time-consuming.
SVM [68]	- Effective in high-dimensional spaces. - Memory efficient; uses a subset of training points. - Robust performance with various kernel functions.	- Requires optimal kernel selection. - Can struggle with noisy and large datasets. - Computationally intensive with many support vectors.
DNN [69], [70]	- Excellent feature learning capabilities, automatically detecting intricate patterns in fault data. - Enhanced modeling of nonlinear relationships, crucial for complex network topologies.	- Large labeled datasets are required for optimal training. - Prone to overfitting if not properly regularized. - Much more computationally intensive than other methods.

where R_f signifies the resistance at the fault, I_f denotes the fault current, D represents the distance to the fault location, and Z_{ab} and Z_{ac} are the inductance between a, b and a, c phases, respectively. The fault current is determined by the difference in the phase current before and after the fault event, as captured by the flow at the inception of the line:

$$I_f = I_a - I_{a'}, \tag{3}$$

where the linear flow $I_{a'}$ on the faulted phase post-fault is a critical parameter for system analysis.

It is worth noting that within the architecture of a radial distribution network, the linear flow subsequent to the fault incident can be determined by employing a radial load distribution algorithm. This calculation is predicated on the voltage present at the fault point, as denoted as follows:

$$I_a = f(V_a, V_b, V_c), \tag{4}$$

where the linear flow I_a on the faulted phase post-fault is a function f of the voltages V_a, V_b, V_c at the fault point. The phase currents and the distance to the fault can characterize the fault point voltages. The determination of the fault current involves the following steps:

1) Commencing with an initial presumption of fault current I_f, an iterative process is employed. The fault current is given by:

$$I_f = I_a - I_{a,pre}, \tag{5}$$

where $I_{a,pre}$ represents the pre-fault current in phase 'a' of the distribution system. This is the current flowing in phase 'a' immediately before the occurrence of the fault. The significance of $I_{a,pre}$ lies in its role as a baseline or reference value against which changes due to the fault are measured.

2) Once the fault current has been ascertained, one may extract the fault distance and resistance. This extraction is facilitated by segregating the fundamental equation into its constituent real and imaginary parts and resolving the subsequent real equation.
3) The voltage fault and, consequently, the voltage vector at the fault point are computed based on the previously mentioned equation.
4) Utilizing the calculated voltage vector, the linear flow post-fault is again obtained via the radial load distribution algorithm. The fault location algorithm's pivotal component is the post-fault flow computation, achieved through the radial load distribution algorithm.

In the described fault location algorithm, a fundamental assumption is made regarding the accessibility of specific values at the conclusion of the faulted section. The approach incorporates a method designed to compute the voltages and currents at the beginning of each line section $(i + 1)$ where a fault has occurred as follows:

$$V_{abc,i} = V_{abc,s} - \sum_{j=1}^{i} Z_{abc,i} I_{abc,j}, \tag{6}$$

where V_{abc} is the voltage vector at the post and Z_{abc} is the impedance matrix of the i^{th} line segment. I_{abc} denotes the current vector in the i^{th} line segment which can be calculated as follows:

$$I'_{abc} = I'_{abc,s} - \sum_{k=1}^{j-1}[I_K], \tag{7}$$

where I_{abc} indicates the measured current vector in the post and I_k represents the load current to the bass k. The parameter I_k can be calculated using a radial load distribution algorithm.

Remark 1: Given that the distribution feeder, structured as a radial network with numerous branches, is linked to the main feeder, faults occurring at various points can result in identical voltage and current readings at the post-fault stage. This means that using the post-fault values, which are crucial for determining the fault's location, can lead to multiple potential fault locations. Hence, the initial step in the fault location process involves identifying all these potential fault sites. A thorough examination of the network is required to address this challenge, which involves applying the fault location algorithm in a segmented manner and systematically analyzing each part of the network. Accordingly, the algorithm can more accurately detect the specific segment where the fault has occurred despite the similar post-fault readings that may be observed across different locations.

During the fault analysis process, the voltage and current measurements at the base, denoted as n, are accurately assessed up to the point where the fault has occurred in the line section. Apart from the fault current in the affected phase, other factors influence the accuracy of the fault distance calculation at base n. These factors stem from the uncertain values amidst the voltage and current data. Hence, (6) and (7) can be rewritten specifically for the faulted phase as:

$$I = I_s - \sum_{k=1}^{n} I_k, \tag{8}$$

$$V = V_s - I_s \sum_{k=1}^{n} Z_k L_k + \sum_{k=1}^{n-1}(n-k) I_k Z_{k+1} L_{k+1}. \tag{9}$$

The correlation between the voltage and current at the endpoint of the line section where the fault is situated can be represented as:

$$V = (I - I')R_f + DZI. \tag{10}$$

Separating (10) into real and imaginary parts and solving them for the fault distance yields,

$$D = \frac{V_r I_i - V_r I'_i - V_i I_r + V_i I'_i}{I_i I'_i Z_i + I_r I'_r Z_i - I_r I'_i Z_r + I_i I'_r Z_r - I_i^2 Z_1 - I_r^2 Z_i}, \tag{11}$$

where r represents the real part, and i denotes the imaginary part. The values I_i, I_r, V_i, V_r are obtained by separating the complex equation into two distinct real equations.

Furthermore, distribution networks extensively utilize smart electronic devices for various functions, including protection, monitoring, and other critical operations. These functions encompass smart measurement systems such as smart sensors, power quality monitoring, and the automation of distribution systems. Their placement spans from the primary distribution post all the way to the consumers' locations, ensuring comprehensive monitoring and control. A diverse array of these smart electronic devices, along with their respective applications, is exemplified in Fig. 3, providing a clear understanding of the different types of devices in use and how they contribute to the overall functionality and efficiency of the distribution network.

III. PROPOSED FAULT LOCALIZATION APPROACH

This work presents an innovative approach to fault location in distribution networks, emphasizing an ANN-based strategy and considering fault impedance. The fundamental concept of the proposed scheme involves segmenting the distribution network into various zones. These zones are defined based on the geographical positioning and generation capacity of DG units in conjunction with the network loads. Each zone begins at the start of a feeder and encompasses an area that each DG unit can support in terms of the average load. The demarcation of a zone concludes when the cumulative load of the posts within it exceeds the generation capacity of the corresponding DG unit. In scenarios where a subsequent DG unit falls within the feeding range of an existing zone, and the aggregate load remains within the first DG unit's capacity, the zone's boundary is expanded to include this additional DG unit. In zones devoid of DG units or where a balance between generation and consumption is achievable based on the average load, this equilibrium is maintained independently from the main network, relying solely on the generation capacity of the DG units within that zone. Subsequent to the zoning process and boundary determination, the system incorporates multiple circuit breakers capable of swift and frequent operations positioned between the zones.

In order to implement the proposed protective approach, a sophisticated computer-based relay, endowed with high processing power and substantial storage capacity, is installed at each feeder post within the distribution network. To facilitate load-shedding operations, switches equipped with a shunt trip mechanism for remote tripping are integrated, allowing connectivity to the main relay. Figure 4 illustrates the developed scheme, and Fig. 5 depicts the distribution network diagram featuring computer-based relays together with the shunt trip switches.

The developed scheme is based on accurately identifying both the type and location of faults within the protective zones. In this work, four multilayer perceptron (MLP) ANNs are trained using data derived from system modeling and short circuit analysis performed across various locations with differing fault impedances. These offline calculations enable the main relay to accurately detect the type and location of faults in real time. This method bifurcates into two critical segments: diagnosing the fault type and pinpointing its location, leveraging the capabilities of ANNs to enhance

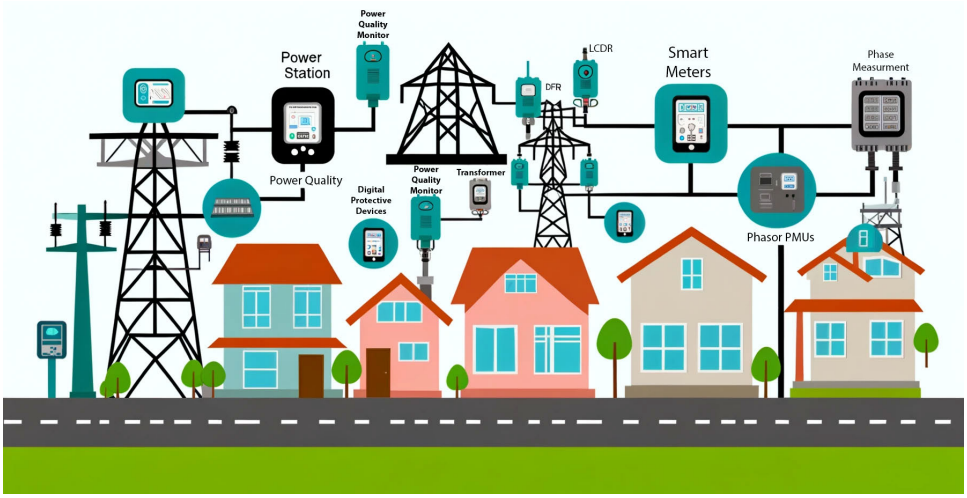

FIGURE 3. Illustration of smart electronic devices in a distribution network.

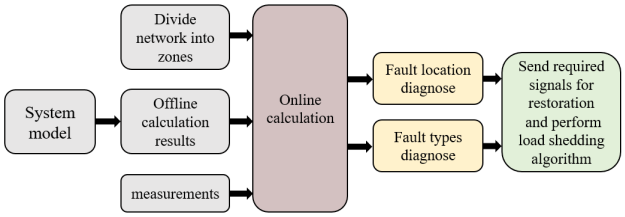

FIGURE 4. Illustration of the developed scheme.

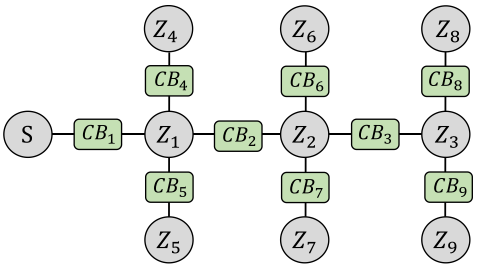

FIGURE 5. Distribution network diagram featuring computer-based relays and shunt trip switches for enhanced protective operations. Z_i: impedance, CB_i: circuit breaker, and S: Electric power source.

fault location accuracy in distribution networks, especially considering the variable fault impedances. In this study, a comprehensive model of the distribution network using DIgSILENT PowerFactory software has been developed, incorporating essential components such as lines, buses, transformers, and generation sources. Faults at various network locations have been introduced, varying the impedance values (0, 50, 100, and 150 ohms) to simulate a range of fault conditions. The software captured key system responses such as current and voltage during each scenario, which were then processed and normalized to form a consistent dataset for ANN training. Subsequently, this dataset was utilized to train multiple MLP-ANNs, each customized to a specific fault type, thus enhancing the models' ability to accurately localize faults under diverse conditions. Algorithm 1 illustrates the developed ANN-based fault localization training procedure.

A. FAULT LOCATION DETERMINATION

The developed approach utilizes the power supply's three-phase current to ascertain the specific fault type. At this juncture, the deployment of an ANN is not required. Instead, the determination is achieved by normalizing the three-phase

Algorithm 1 ANN-Based Fault Localization Training Procedure

```
Define Z_imp ← [0, 50, 100, 150] Impedance values in ohms
Define F ← {Fault locations}
Define N ← Set of network components
procedure Generate Training Data(N, Z_imp, F)
    Initialize PowerFactory software
    NetworkModel ← MODELNETWORK N
    for each f ∈ F do
        for each z ∈ Z_imp do
            Simulate Fault (f, z)
            [I, V] ← Get System Responses (f)
            I_norm, V_norm ← Normalize (I, V)
            Data_ANN ← Data_ANN ∪ {(I_norm, V_norm)}
    return Data_ANN
procedure Train ANN(Data_ANN)
    for each fault type ∈ {Three-phase, Single-phase, etc.} do
        ANN ← Initialize MLP Structure (fault type)
        Train MLP (ANN, Data_ANN)
        Validate and save ANN
TrainingData ← GENERATE TRAINING DATA N, Z_imp, F
TRAIN ANN TrainingData
```

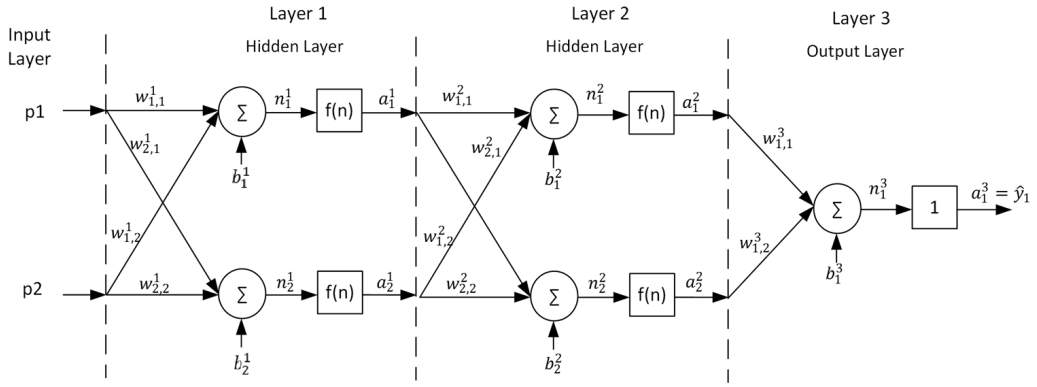

FIGURE 6. Schematic of an MLP-ANN structure.

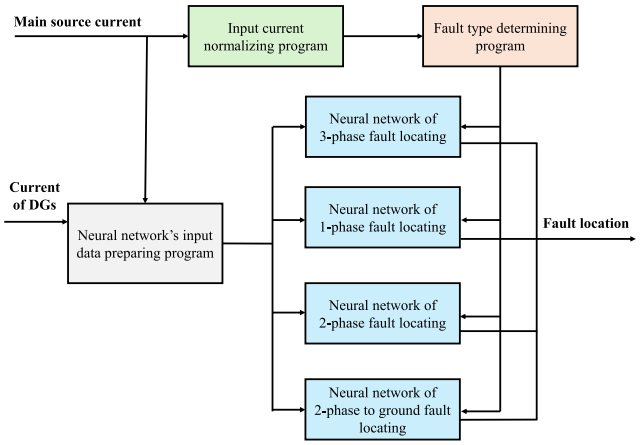

FIGURE 7. The developed fault-location method.

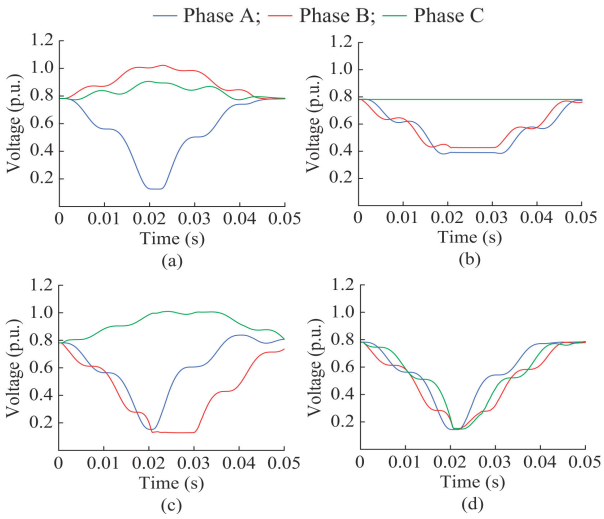

FIGURE 8. Illustration of voltage signals for various fault types. (a) Phase-A-to-ground (Ag). (b) Phase-A-to-phase-B (AB). (c) Two-phases-to-ground (ABg). (d) Three phases (ABC).

current output at the feeder post. In this context, its exact location must be identified once the error type is determined. In this study, an MLP-ANN —whose structure is depicted in Fig. 6— is integrated for accurately locating the fault. A brief overview of the developed fault-location method is illustrated in Fig. 7. Following the detection of the fault type by the respective unit, the specifically trained ANN for this fault type becomes operative and processes the input data, which the input data preparation program has prepared. The output from the ANN indicates the fault's proximity to all DG units and the primary supply. Furthermore, to reduce the influence of fault impedance on the ANN's output, it is necessary to define suitable features for the MLP-ANN. The incorporated ANN considers the proportional relationship between the DGs' fault current and the feeder substations as its input. Considering (2)-(5), the normalization process yields,

$$I_{normal} = \frac{I}{I_{max}} \tag{12}$$

where I indicates the phase current and I_{max} represents the maximum phase current. The fault type can be identified using (12). Four fault types are considered in this study; a) one phase to the ground, b) phase-to-phase contact, c) two phases to the ground, and d) three-phase contact, as detailed in Table 2, where the voltage signals for various fault types are depicted in Fig. 8.

TABLE 2. The normalized vector of feeding current for different faults.

	Fault type	Ia	Ib	Ic
Single phase	Ag	0	0	1
	Bg	0	1	0
	Cg	1	0	0
Two phase	AB	0	-1	1
	AC	-1	0	1
	BC	-1	1	0
Two phase to ground	ABg	0	1	1
	ACg	1	0	1
	BCg	1	1	0
Three phase	ABC	1	1	1

Once the fault type has been identified, the next step is to pinpoint its location. The ANN's output yields the fault's distance relative to all DG units and the main feeder. As previously highlighted, a significant challenge in locating faults within distribution networks is the influence of fault

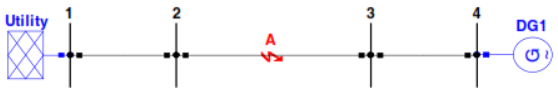

FIGURE 9. Illustration of a sample network with fault.

impedance. To mitigate the impact of fault impedance on the ANN's output, it is essential to define suitable characteristics for the ANN. In addition, an important factor considered in the ANN's input is the proportional relationship between the fault current from the DGs and the currents at the feeder posts. The fault current contribution from each DG is computed using (3)-(5). Considering V as the power supply terminal voltage and Z_{th} as the equivalent impedance of the network tune, one has

$$I_f = \frac{V}{Z_{th}}. \tag{13}$$

Consider the network illustrated in Fig. 9. In a scenario where a short circuit occurs and is characterized by zero resistance, the computation of the equivalent impedance involves both the DG and the overall network as follows:

$$Z_{DG} = Z_{34} + Z_{3a}, \tag{14}$$
$$Z_S = Z_{12} + Z_{2a}, \tag{15}$$

where Z_{12} and Z_{34} are the impedance of the transmission line between buses 1 and 2, and buses 3 and 4, respectively. Z_{3a} represents the impedance of the transmission line between bus 3 and point A (fault point), and Z_{2a} is the impedance of the transmission line between bus 2 and the point A (fault point) shown in Fig. 9.

In this network, the ratio of the network short-circuit current to the DG short-circuit current is equal to:

$$\frac{I_S}{I_{DG}} = \frac{Z_{34} + Z_{3a}}{Z_{12} + Z_{2a}}. \tag{16}$$

By assuming a short-circuit non-zero impedance at point A, the implied relation is obtained as follows:

$$\frac{I_S}{I_{DG}} = \frac{Z_{34} + Z_{3a} + Z_f}{Z_{12} + Z_{2a} + Z_f}. \tag{17}$$

This observation is congruent with the estimation provided in (16). By employing this specific ratio—the ratio representing the relationship between the injected fault current from various sources and the input to the ANN—the impact of fault impedance is minimized. Moreover, it is noteworthy that augmenting the number of DG units linked to the distribution system enhances the precision of fault location determinations made by the ANN. The transfer function for the output neurons is linear, and hyperbolic tangent types are used for the hidden neurons. In order to train the ANN, the Levenberg-Marquardt algorithm is adopted, which is a sophisticated approach that combines the concepts of gradient descent and Gauss-Newton methods. The Levenberg-Marquardt algorithm iteratively adjusts the weights of the network to minimize the error between the predicted and actual outputs. The adjustment is made according to the equation:

$$\Delta_w = -(J^T J + \lambda I)^{-1} J^T r, \tag{18}$$

where Δ_w represents the change in weights, J is the Jacobian matrix containing first derivatives of the network errors with respect to the weights, r is the vector of residuals (differences between actual and predicted outputs), λ denotes a damping factor that adjusts the algorithm's behavior between the gradient descent and Gauss-Newton methods, and I represents the identity matrix. The algorithm is sensitive to the choice of λ; a higher λ makes the algorithm behave more similar to gradient descent, providing more robustness in the presence of poor initial weight estimates, while a lower λ leans towards the Gauss-Newton method, favoring faster convergence when close to the minimum error.

B. FAULT ISOLATION AND NETWORK RECOVERY

The method developed in this work aims to segregate the faulted sector from the operational segments of the network by activating the circuit breakers that delineate the feeder network zones. Upon identifying the fault's location and type, a shedding signal is dispatched to the circuit breakers within and downstream of the faulted area. Additionally, for zones equipped with DG units, the relay issues a shutdown command to all such units within the impacted area. As a result, the faulted zone experiences a power outage, its electrical continuity with other parts of the network is severed, and areas upstream maintain synchronized operation with the main network. Meanwhile, downstream zones are either powered through the independent operation of their DG units, if available, or face a disruption in power supply.

The process of re-establishing the connection involves the isolation switches, which are operated via the main power relay control. The protocol dictates that reconnection is executed once the faulted section is isolated by bridging the affected zone back to the upstream network upon the main relay's command. Subsequent to each reconnection attempt, the relay evaluates the network's condition. In this context, should the fault persist, the relay reissues the interrupt command. Conversely, if the fault is transient and clears during the reconnection attempt, the relay initiates commands to restore network function. To illustrate, refer to Fig. 5, where a transient fault in zone Z_2 prompts the relay to initially halt circuits at CB_2, CB_3, CB_6, CB_7, CB_8, CB_9, and all DGs in Z_2. The relay then attempts reconnection at CB_2, detecting the transient nature of the fault. Ultimately, once the fault is cleared, the relay commands the re-synchronization and reconnection of CB_3, CB_6, CB_7, CB_8, CB_9, and all DGs in Z_2, thereby fully restoring the network.

$$\Delta P = \sum P_{CB_i} \tag{19}$$
$$\Delta Q = \sum Q_{CB_i} \tag{20}$$

C. LOAD SHEDDING

As the network loading exceeds the average and a system malfunction arises, certain network regions might engage in islanding operations post-network restoration. Consequently, load shedding becomes essential in these areas. This study's approach calculates the load variance in each zone by summing the current flows through isolation switch zones immediately preceding the fault. By using (19) and (20) to ascertain ΔP and ΔQ for every zone, one can evaluate the mismatch or surplus relative to each zone's generation capacity. Subsequently, load shedding can be strategically executed by incorporating anticipated hourly load profiles, fault timing, ΔP, ΔQ, and the importance of the loads.

IV. SIMULATION RESULTS

The proposed approach was validated using a test system comprising a $20KV$, 22-bus grid equipped with a $3.5MWA$ diesel generator connected to the 22-bus and a $4.5MWA$ diesel generator linked to the 4-bus is considered. Fig. 10 illustrates the network's single-line diagram. Table 3 demonstrates the technical specifications of the distributed generation sources, where X_d and X_q are the generators' d-axis and q-axis synchronous reactances, and X'_d and X''_d represent the generators' d-axis transient and subtransient reactances, respectively. The single-line diagram of the distribution feeder post-application of the zoning methodology augmented with circuit breakers and their positioning for dividing the network into protective zones is depicted in Fig. 11. The zoning procedure results in a feeder divided into four zones, including two zones equipped with DG capable of islanding operation. These zones are demarcated from each other by circuit breakers CB_1, CB_2, CB_3, and CB_4. To gather the requisite data for training the ANN and conducting offline computations, simulations of various system faults were carried out at 100-meter intervals, incorporating fault impedances of 0, 50, 100, and 150 ohms, and the output current from all feed resources was recorded. The maximum load for all load types was set at 1 MW, with a consistent power factor of 0.92 across all hours. The specific ANN configurations for each fault type are detailed in Table 4. The implemented MLP-NN holds 18 weights between the input and hidden layers (W_{i-h}), 6 biases in the hidden layer (b_h), 18 weights between the hidden and output layers (W_{h-o}), and 3 biases in the output layer (b_o) chosen as follows:

$$W_{\text{i-h}}^{T} = \begin{bmatrix} 0.11 & -0.45 & 0.34 & -0.29 & 0.07 & 0.55 \\ 0.43 & -0.12 & 0.23 & -0.67 & 0.35 & -0.10 \\ -0.22 & 0.29 & -0.56 & 0.25 & -0.38 & 0.47 \end{bmatrix},$$

$$b_{\text{h}} = \begin{bmatrix} 0.05 & -0.07 & 0.09 & 0.03 & -0.02 & 0.04 \end{bmatrix},$$

$$W_{\text{h-o}}^{T} = \begin{bmatrix} -0.31 & 0.19 & 0.04 & -0.12 & 0.49 & -0.31 \\ 0.27 & -0.55 & 0.11 & 0.58 & -0.43 & 0.17 \\ -0.48 & 0.66 & -0.22 & -0.01 & 0.28 & -0.74 \end{bmatrix},$$

$$b_{\text{o}} = \begin{bmatrix} 0.10 & -0.05 & 0.03 \end{bmatrix}$$

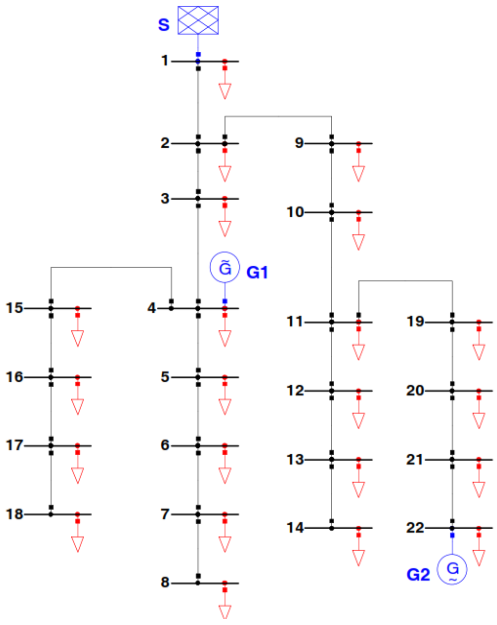

FIGURE 10. Illustration of the modeled network.

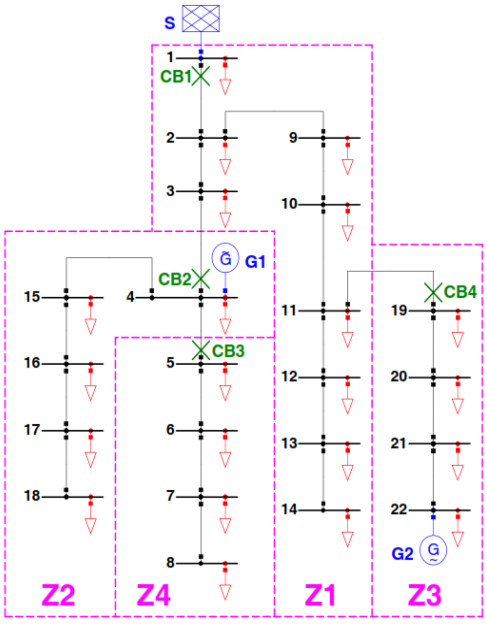

FIGURE 11. Illustration of the zones and the determined boundaries.

A. PERFORMANCE EVALUATION AND VALIDATION

To evaluate the effectiveness of the developed protection and location method, and illustrate the operation sequence of the main relay in the event of a fault along the feeder, we analyzed the performance of the MLP-ANN in zones 1 through 4, as depicted in Figs. 12-15, respectively. Figures 12-15 demonstrate the learning curves for the MLP-ANN model, plotting the mean squared error (MSE) against epochs for training, validation, and test datasets across four different faulty scenarios of three-phase, single-phase, two-phase, and two-phases to the ground. As one can observe from Fig. 12,

TABLE 3. Technical information of DGs.

Data	Value	Unit
Type of Machine	IEC 909	-
Voltage	20	kV
Nominal power	2.8 & 3.6	MW
Nominal power coefficient	0.8	–
Connection	YN	-
X_d	1.5	pu
X_q	0.75	pu
X'_d	0.256	pu
X''_d	0.168	pu

TABLE 4. ANN structure for each fault type occurrence.

Type of fault	ANN structure
Three Phases	[3 6 3]
Single Phase	[3 5 3]
Two phases	[3 7 3]
Two phases to the ground	[3 7 3]

TABLE 5. Fault zone location error percentage for different fault scenarios.

	Fault type	Fault impedance (ohm)	Error (%)
Single-phase	Ag	50	0.0015
	Bg	100	0.0053
	Cg	150	0.0068
Two-phase	AB	50	0.018
	AC	100	0.022
	BC	150	0.039
Two-phase to ground	ABg	50	0.15
	ACg	100	0.24
	BCg	150	0.27
Three-phase	ABC	100	0.36

for Zone 1 and Zone 4, the best validation performance is observed at epochs 2 and 1, respectively, which suggests that the models quickly find a generalized solution. Zone 2 and Zone 3's best performances are identified at epochs 3 and 1, respectively, showing early model convergence. After the initial epochs, the MSE stabilizes across all zones, indicating minimal gains from additional training epochs. This consistent pattern of early convergence in all zones suggests that the developed ANN effectively captures the underlying patterns for fault localization tasks with high efficiency.

To elaborate further on the accuracy evaluation of the proposed fault-detection method, several types of faults including one phase to the ground, phase-to-phase contact, two phases to the ground, and three-phase contact have been simulated and analyzed, with their respective fault impedance and error percentages detailed in Table 5. The results demonstrate that the presented method maintains high accuracy, and its performance is unaffected by variations in resistance.

On the other hand, as it can be seen in Fig. 13, a quick learning within the first few epochs in Zone 1 is observed and the best validation performance emerges at epoch 4, suggesting that the model reaches a good level of generalization early on. In contrast, Zone 2's model appears to learn at a similar pace but achieves its best validation performance much later, at epoch 24, which could indicate overfitting or a need for more complex learning as

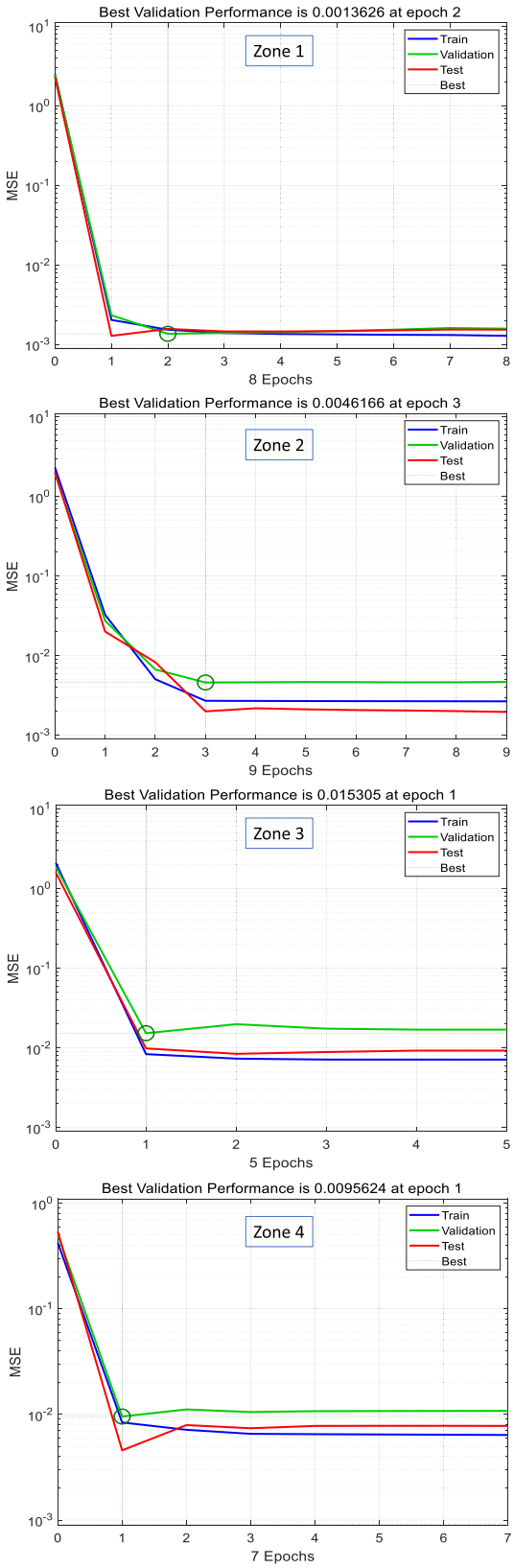

FIGURE 12. MLP-ANN fault localization for three-phase faults in zones 1 through 4.

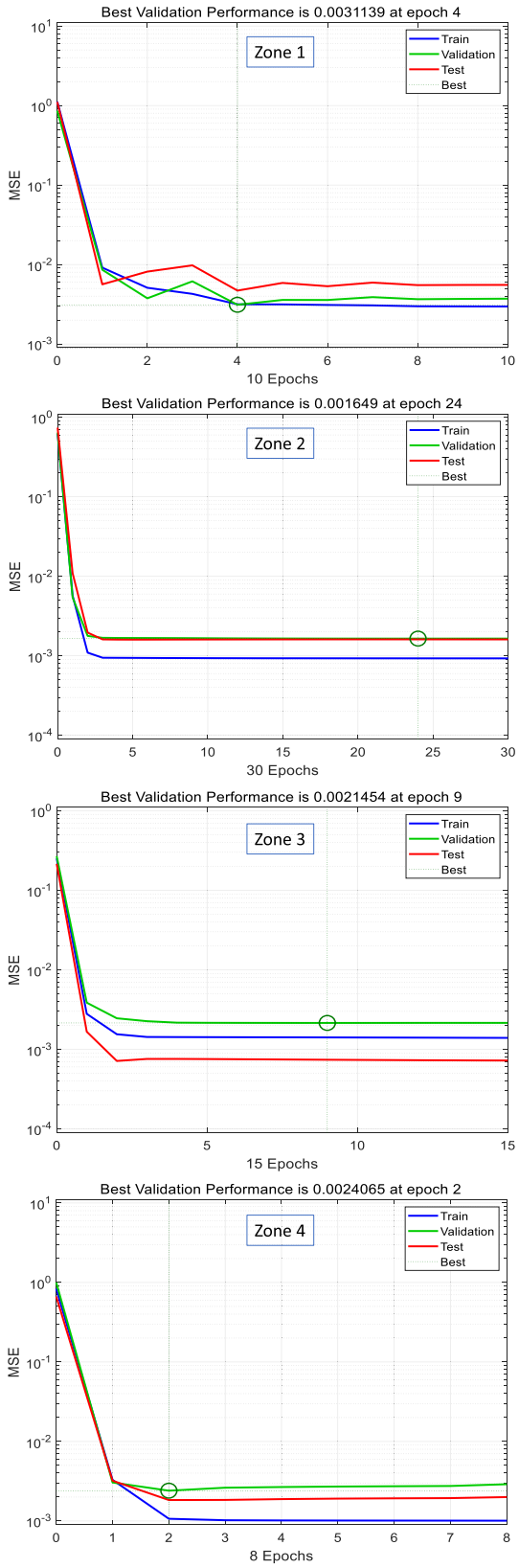

FIGURE 13. MLP-ANN fault localization for single-phase faults across zones 1 through 4.

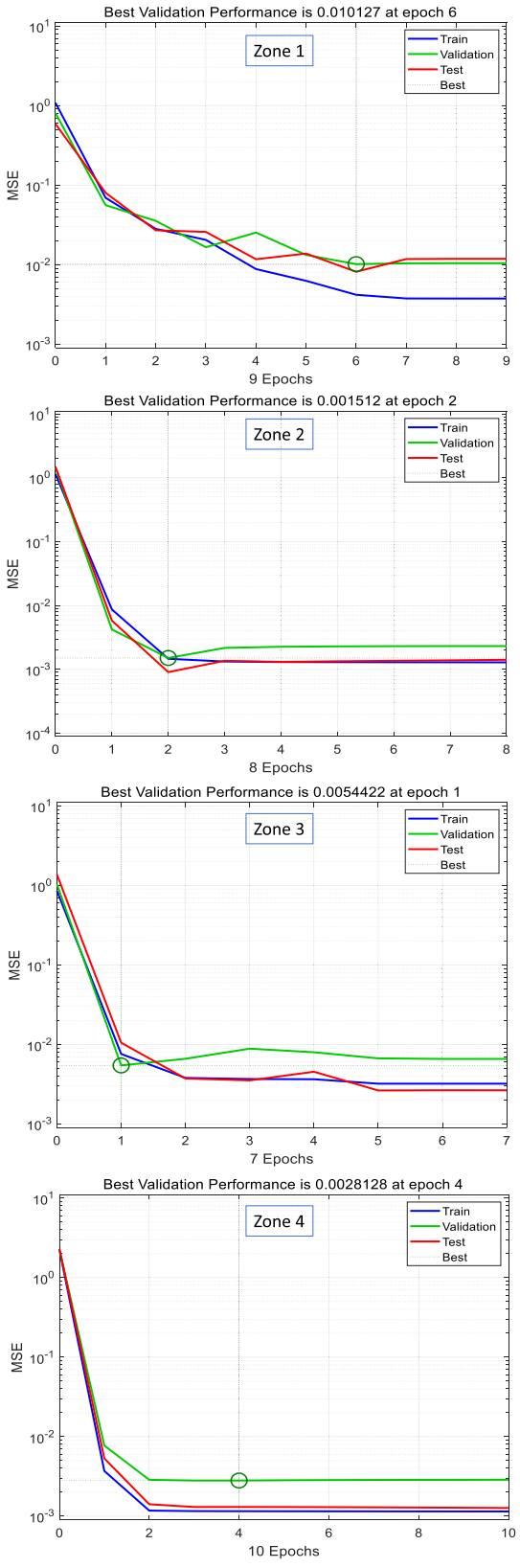

FIGURE 14. MLP-ANN fault localization for two-phase faults in zones 1 through 4.

epochs progress. Zone 3's model exhibits a more gradual improvement, not stabilizing as quickly as the others, with the best validation performance occurring at epoch 9, which could suggest a more challenging fault localization task in this zone. Also, Zone 4's model learns quickly, with the best performance at epoch 2, and similar to Zone 1, it does not show significant improvements after the initial epochs, pointing to a swift convergence to an optimal solution.

From the two-phase fault type localization shown in Fig. 14, it can be observed that Zone 1 and Zone 3 reach their best validation MSE later in the training process, at epochs 6 and 1, respectively, with Zone 1 showing some fluctuation in MSE before stabilizing. Zone 2 and Zone 4 demonstrate rapid learning, with the best validation MSE appearing as early as epoch 2 and 4, respectively, and MSE stabilizing shortly after. This behavior across the zones implies that while the model is capable of rapidly understanding the fault localization task, the faults' complexity or nature may vary between zones, affecting the speed and stability of the learning process. Furthermore, Fig. 15 demonstrates the localization of two phases to the ground fault type, at which Zone 1 and Zone 2 exhibit a quick decline in MSE, with the best validation performance achieved at epoch 3 and epoch 2, respectively, indicating an effective and rapid learning process. Zone 3 is unique, with its best validation performance occurring much later at epoch 17, suggesting that the model required more iterations to adequately capture this zone's fault characteristics. Zone 4's learning curve quickly plateaus, with the best performance at epoch 1, which implies immediate model effectiveness. Table 6 and Fig. 16 illustrate the MSE values for each zone with various fault types. The data regression diagram for the training, validation, and test datasets for the four fault scenarios is depicted in Fig. 17. The scatter plots depict a predictive model's performance under four different conditions, showing a strong linear relationship between predicted outputs and actual targets.

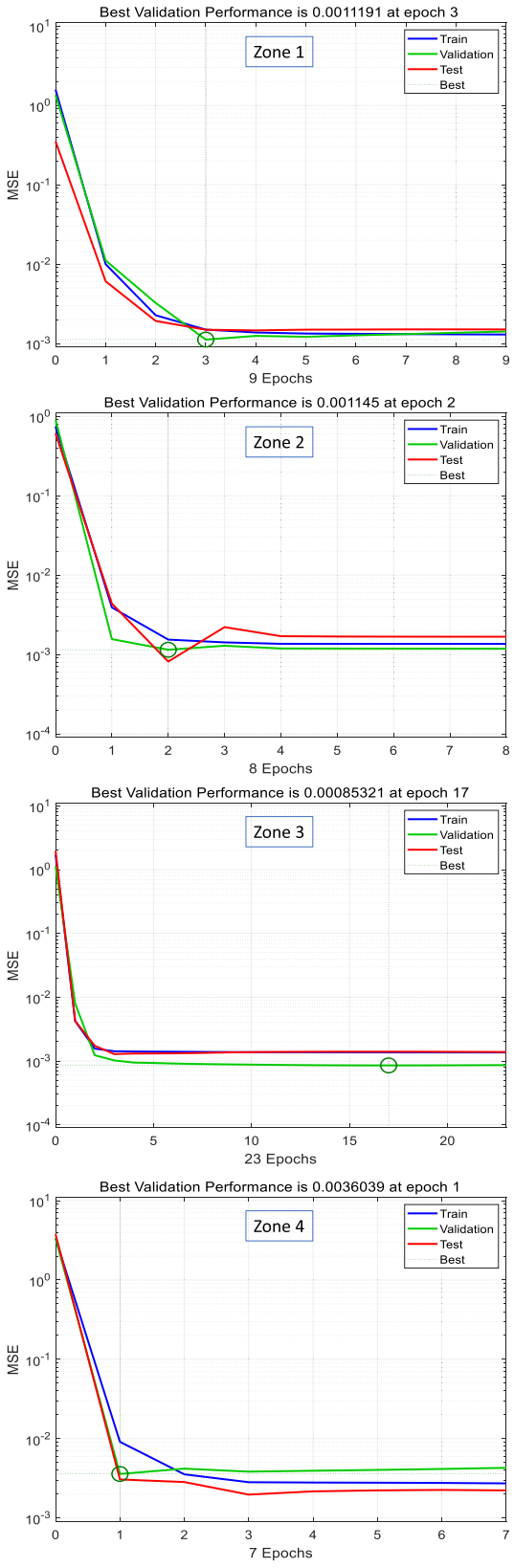

FIGURE 15. MLP-ANN fault localization for two-phase to the ground faults across zones 1 through 4.

B. PERFORMANCE VERIFICATION FOR SIGNAL INTERFERENCE

In practice, data acquisition devices are affected by varying levels of noise or data loss due to different working conditions. Hence, the ability to perform well across different situations is a key aspect of the fault diagnostic model. This study investigates the effectiveness of the proposed approach under different noise conditions arising from electromagnetic interference and other environmental elements. Accordingly, Gaussian white noise is used to simulate the impact of these environmental factors. The signal noise ratios (SNRs) of the data are set at 10, 15, 25, and 35 dB. The effects of various SNRs on the voltage signals depicted in Fig. 8 are depicted in Fig. 18. The accuracy results for fault location of the proposed method are compared with that of graph convolutional network (GCN) [72] under various SNRs, in Fig. 19. It is evident that the GCN approach is highly affected by noise, whereas the proposed

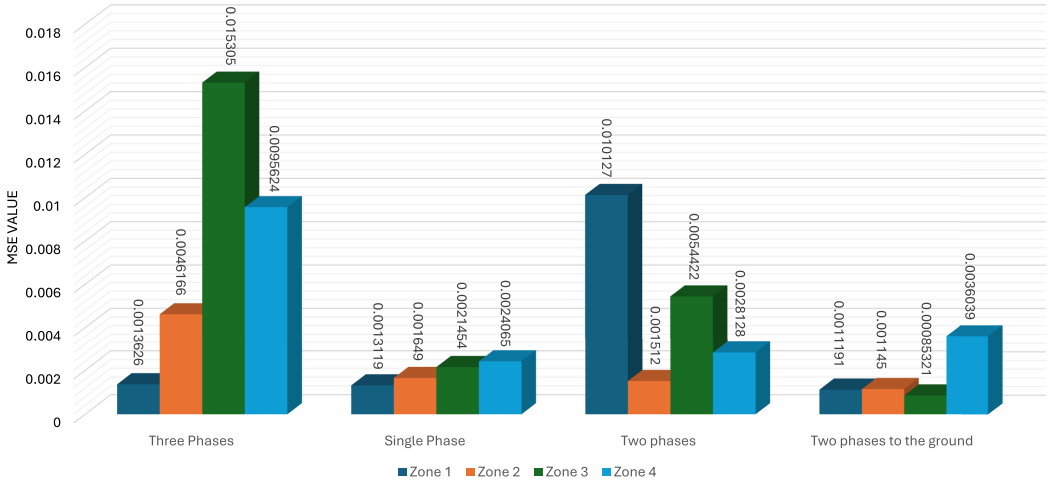

FIGURE 16. MSE value demonstration of different zones for each fault type.

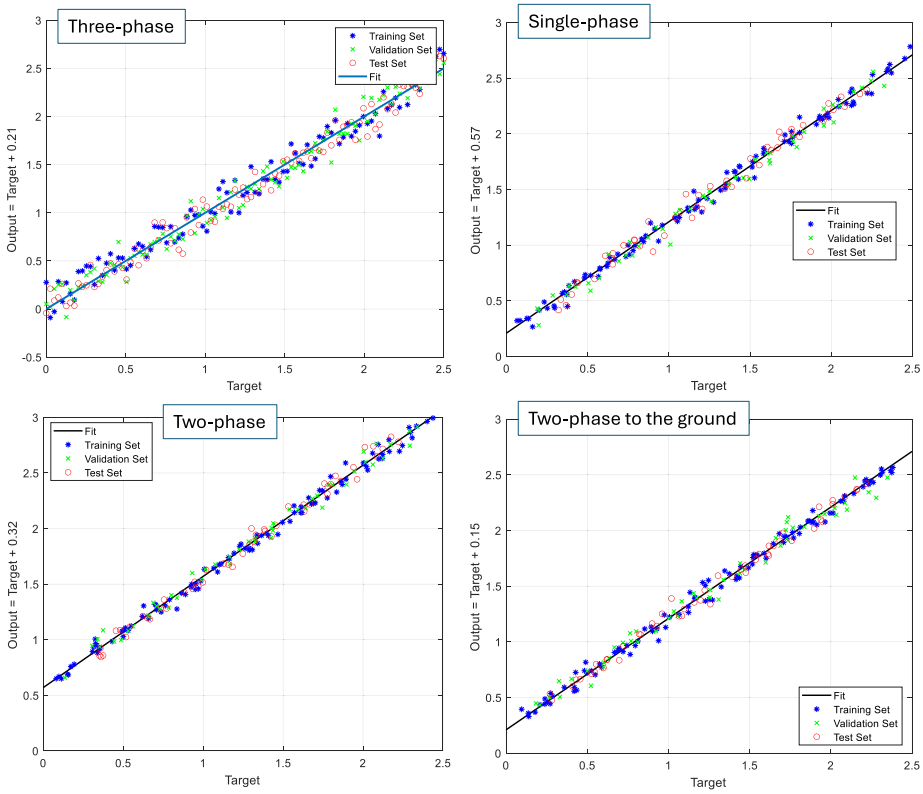

FIGURE 17. Data regression diagram illustration of the MLP-ANN in four fault scenarios.

TABLE 6. MSE value of different zones for each fault type.

Type of fault	MSE value							
	Zone 1	Ep.	Zone 2	Ep.	Zone 3	Ep.	Zone 4	Ep.
Three Phases	0.0013626	2	0.0046166	3	0.015305	1	0.0095624	1
Single Phase	0.0013119	4	0.001649	24	0.0021454	9	0.0024065	2
Two phases	0.010127	6	0.001512	2	0.0054422	1	0.0028128	4
Two phases to the ground	0.0011191	3	0.001145	2	0.00085321	17	0.0036039	1

TABLE 7. Advantages, disadvantages, and future prospects of the proposed fault location and protection method.

Aspect	Details
Advantages	1. Enhanced Fault Localization: Precise identification of fault locations using neural networks. 2. Reduction in System Downtime: Efficient fault isolation minimizes network interruptions. 3. Improved Network Reliability: Zoning strategy and DG integration bolster system stability. 4. Optimized Protective Mechanisms: Tailored response to varying fault impedances.
Disadvantages	1. Complexity of Implementation: Requires sophisticated relay systems and network segmentation. 2. Training and Maintenance Costs: High initial investment in system training and maintenance. 3. Data Dependency: Reliance on extensive data for accurate neural network training. 4. Potential for Overfitting: Neural network models may overfit if not properly managed.
Future Prospects	1. Integration with Smart Grid Technologies: Enhanced fault management through smart grid integration. 2. Adaptation to Larger Networks: Scaling up the system for larger and more complex networks. 3. Real-time Data Analysis: Incorporating real-time analytics for quicker fault response. 4. Machine Learning Enhancements: Leveraging advancements in machine learning for improved accuracy.

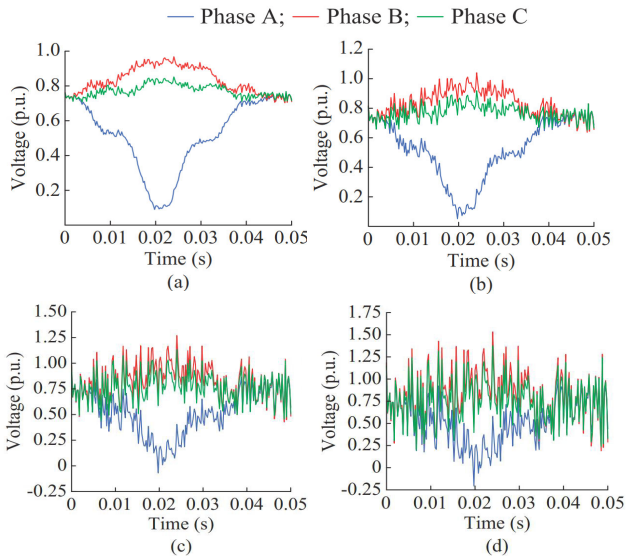

FIGURE 18. Effects of various SNRs on voltage signals. (a) SNR: 35 dB. (b) SNR: 25 dB. (c) SNR: 15 dB. (d) SNR: 10 dB.

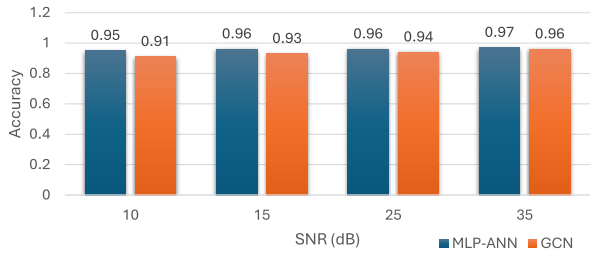

FIGURE 19. Comparative fault location accuracy analysis under various SNRs; proposed vs GCN.

method achieves good performance despite the presence of noise.

V. CONCLUSION

This study introduced a novel fault location and protection method for distribution systems with DG, utilizing a multi-layer perceptron neural network. Central to our approach was the implementation of a zoning strategy, which partitioned the distribution system into multiple independent sections, each capable of islanding operation. This zoning facilitated a more organized and effective fault management process. Upon segmentation, a high-capacity computer-based relay was installed at each feeder post, playing a crucial role in monitoring the network and accurately determining fault locations using the ANN, which was pre-trained through extensive offline simulations. The relay's critical function was to identify faults and issue commands to isolate the affected zone, thereby safeguarding network devices and maintaining system integrity.

The results of the implemented ANN training demonstrate its efficacy, with an optimal performance in fault detection and localization. The system's capability to isolate faults effectively minimized downtime and enhanced the reliability of the power distribution network. Additionally, the zoning concept not only simplified fault management but also contributed to the overall stability and efficiency of the network, especially in scenarios involving DGs. One of the key accomplishments of this research is the development of a system that adeptly handles the complexities introduced by DG integration. The method effectively addressed the challenges posed by fault impedance variations and ensured precise fault localization, thereby optimizing the response time and accuracy of the distribution system's protective mechanisms. The advantages, disadvantages, and future prospects of the proposed fault location and protection method are illustrated in Table 7.

In future works, the distinct operational dynamics of various types of DG sources, such as renewable energy systems and storage devices, and their implications for fault detection and location will be investigated. The main goal would be to explore diverse fault response behaviors influenced by both the nature of the energy source and the interlinking power electronics. This exploration will lead to the development of a comprehensive protection scheme that is cognizant of these variances. Furthermore, the complexities introduced by the variability of renewable sources and their control systems will be tackled, which will involve enhancing the analytical models to factor in the influence

of power electronic interfaces on fault current magnitudes and profiles. Moreover, the study will also expand to include a detailed evaluation of islanding operations within the network, evaluating the stability and reliability of the power supply during and after fault conditions. The efforts will be directed toward improving the predictive capabilities of the system by incorporating real-time data analytics to enhance fault detection accuracy and optimize response strategies.

REFERENCES

[1] S. S. Gururajapathy, H. Mokhlis, and H. A. Illias, "Fault location and detection techniques in power distribution systems with distributed generation: A review," *Renew. Sustain. Energy Rev.*, vol. 74, pp. 949–958, Jul. 2017.

[2] A. Sohani, H. Sayyaadi, S. R. Miremadi, S. Samiezadeh, and M. H. Doranehgard, "Thermo-electro-environmental analysis of a photovoltaic solar panel using machine learning and real-time data for smart and sustainable energy generation," *J. Cleaner Prod.*, vol. 353, Jun. 2022, Art. no. 131611.

[3] F. Pazhoohesh, S. Hasanvand, and Y. Mousavi, "Optimal harmonic reduction approach for PWM AC–AC converter using nested memetic algorithm," *Soft Comput.*, vol. 21, no. 10, pp. 2761–2776, May 2017.

[4] M. E. H. Golshan, S. H. H. Dolatabadi, and S. M. Tabatabaei, "Determining minimum number and optimal placement of PMUs for fault observability in one-terminal algorithms," *IET Gener., Transmiss. Distribution*, vol. 12, no. 21, pp. 5789–5797, Nov. 2018.

[5] S. Naderian and A. Salemnia, "An implementation of S-transform and type-2 fuzzy kernel based support vector machine algorithm for power quality events classification," *J. Intell. Fuzzy Syst.*, vol. 36, no. 6, pp. 5115–5124, Jun. 2019.

[6] Y. Mousavi, M. H. Atazadegan, and A. Mousavi, "Multi-objective power distribution network reconfiguration using chaotic fractional particle swarm optimization," *ECTI Trans. Electr. Eng., Electron., Commun.*, vol. 19, no. 1, pp. 43–50, Feb. 2021.

[7] A. Zarei, Y. Mousavi, R. Mosalanezhad, and M. H. Atazadegan, "Robust voltage control in inverter-interfaced microgrids under plug-and-play functionalities," *IEEE Syst. J.*, vol. 14, no. 2, pp. 2813–2824, Jun. 2020.

[8] D. Chanda and N. Y. Soltani, "A heterogeneous graph-based multi-task learning for fault event diagnosis in smart grid," 2023, *arXiv:2309.09921*.

[9] M. J. Zideh and S. K. Solanki, "Physics-informed convolutional autoencoder for cyber anomaly detection in power distribution grids," 2023, *arXiv:2312.04758*.

[10] M. Tavasoli, S. Alishahi, M. Zabihi, H. Khorashadizadeh, and A. H. Mohajerzadeh, "An efficient NSKDP authentication method to secure smart grid," in *Proc. IEEE Int. Conf. Smart Energy Grid Eng. (SEGE)*, Aug. 2017, pp. 276–280.

[11] E. Jandaghi, X. Chen, and C. Yuan, "Motion dynamics modeling and fault detection of a soft trunk robot," in *Proc. IEEE/ASME Int. Conf. Adv. Intell. Mechatronics (AIM)*, Jun. 2023, pp. 1324–1329.

[12] A. L. da Silva Pessoa and M. Oleskovicz, "Fault location algorithm for distribution systems with distributed generation based on impedance and metaheuristic methods," *Electric Power Syst. Res.*, vol. 225, Dec. 2023, Art. no. 109871.

[13] M. Gholamian and O. Beik, "Coordinate control of wind turbines in a medium voltage DC grid," *IEEE Trans. Ind. Appl.*, vol. 59, no. 5, pp. 1–9, 2023.

[14] S. H. H. Dolatabadi and M. E. H. Golshan, "Fault location observability rules for impedance-based fault location algorithms," *Electric Power Syst. Res.*, vol. 224, Nov. 2023, Art. no. 109771.

[15] A. A. Rostam-Alilou, C. Zhang, F. Salboukh, and O. Gunes, "Potential use of Bayesian networks for estimating relationship among rotational dynamics of floating offshore wind turbine tower in extreme environmental conditions," *Ocean Eng.*, vol. 244, Jan. 2022, Art. no. 110230.

[16] H. Torkaman, E. Zeraatkar, N. Deyhimi, H. H. Alhelou, and P. Siano, "Rearrangement method of reducing fault location error in tied uncompleted parallel lines," *IEEE Access*, vol. 10, pp. 51862–51872, 2022.

[17] B. K. Chaitanya and A. Yadav, "An intelligent fault detection and classification scheme for distribution lines integrated with distributed generators," *Comput. Electr. Eng.*, vol. 69, pp. 28–40, Jul. 2018.

[18] G. Sarfi and M. Kalantar, "Predictive direct power control of doubly fed induction generators to reduce the power ripple during the grid synchronization," *Amer. J. Electr. Power Energy Syst.*, vol. 9, no. 6, p. 97, 2020.

[19] A. Sohani, M. H. Shahverdian, H. Sayyaadi, and D. A. Garcia, "Impact of absolute and relative humidity on the performance of mono and poly crystalline silicon photovoltaics; applying artificial neural network," *J. Cleaner Prod.*, vol. 276, Dec. 2020, Art. no. 123016.

[20] A. Bahrami, F. Soltanifar, P. Fallahi, S. S. Meschi, and A. Sohani, "Energy and economic advantages of using solar stills for renewable energy-based multi-generation of power and hydrogen for residential buildings," *Buildings*, vol. 14, no. 4, p. 1041, Apr. 2024.

[21] K. Chen, J. Hu, and J. He, "Detection and classification of transmission line faults based on unsupervised feature learning and convolutional sparse autoencoder," *IEEE Trans. Smart Grid*, vol. 9, no. 3, pp. 1748–1758, May 2018.

[22] Y. Mousavi, G. Bevan, I. B. Kucukdemiral, and A. Fekih, "Sliding mode control of wind energy conversion systems: Trends and applications," *Renew. Sustain. Energy Rev.*, vol. 167, Oct. 2022, Art. no. 112734.

[23] Y. Mousavi, G. Bevan, I. B. Küçükdemiral, and A. Fekih, "Maximum power extraction from wind turbines using a fault-tolerant fractional-order nonsingular terminal sliding mode controller," *Energies*, vol. 14, no. 18, p. 5887, Sep. 2021.

[24] S. Besati, A. Mosallanejad, and M. Manjrekar, "Control strategy for virtual synchronous generator based on Y-Z source inverter in islanded grids," 2023, *arXiv:2312.06543*.

[25] Y. Mousavi, A. Alfi, I. B. Kucukdemiral, and A. Fekih, "Tube-based model reference adaptive control for vibration suppression of active suspension systems," *IEEE/CAA J. Autom. Sinica*, vol. 9, no. 4, pp. 728–731, Apr. 2022.

[26] N. Asadi, M. Hamzeh, and K. Abbaskhanian, "The impact of DSTATCOM on the small-signal stability of islanded microgrids," in *Proc. 11th Power Electron., Drive Syst., Technol. Conf. (PEDSTC)*, Feb. 2020, pp. 1–7.

[27] T. Khatibi and P. Dezyani, "Proposing novel methods for gynecologic surgical action recognition on laparoscopic videos," *Multimedia Tools Appl.*, vol. 79, nos. 41–42, pp. 30111–30133, Nov. 2020.

[28] S. Talebzadeh and O. Beik, "Spacecraft medium voltage direct-current (MVDC) power and propulsion system," *Electronics*, vol. 13, no. 10, p. 1810, May 2024.

[29] S. Sedayevatan, A. Bahrami, F. Delfani, and A. Sohani, "Uncertainty covered techno-enviro-economic viability evaluation of a solar still water desalination unit using Monte Carlo approach," *Energies*, vol. 16, no. 19, p. 6924, Oct. 2023.

[30] A. Mehrzad, M. Darmiani, Y. Mousavi, M. Shafie-Khah, and M. Aghamohammadi, "An efficient rapid method for generators coherency identification in large power systems," *IEEE Open Access J. Power Energy*, vol. 9, pp. 151–160, 2022.

[31] H. Torkaman, M. Shadaei, N. Deyhimi, and H. Torkaman, "Multi-objective method to ReconFigure radial power distribution system with DGs considering transformer tap-changing," in *Proc. IEEE Int. Conf. Environ. Electr. Eng. IEEE Ind. Commercial Power Syst. Eur. (EEEIC / I&CPS Europe)*, Sep. 2021, pp. 1–4.

[32] Y. Mousavi, A. Alfi, and I. B. Kucukdemiral, "Enhanced fractional chaotic whale optimization algorithm for parameter identification of isolated wind-diesel power systems," *IEEE Access*, vol. 8, pp. 140862–140875, 2020.

[33] A. Mehrzad, M. Darmiani, Y. Mousavi, M. Shafie-Khah, and M. Aghamohammadi, "A review on data-driven security assessment of power systems: Trends and applications of artificial intelligence," *IEEE Access*, vol. 11, pp. 78671–78685, 2023.

[34] W. C. Santos, F. V. Lopes, N. S. D. Brito, and B. A. Souza, "High-impedance fault identification on distribution networks," *IEEE Trans. Power Del.*, vol. 32, no. 1, pp. 23–32, Feb. 2017.

[35] S. Besati, S. Essakiappan, and M. Manjrekar, "A new flexible modified impedance network converter," 2023, *arXiv:2304.07866*.

[36] Y. Q. Chen, O. Fink, and G. Sansavini, "Combined fault location and classification for power transmission lines fault diagnosis with integrated feature extraction," *IEEE Trans. Ind. Electron.*, vol. 65, no. 1, pp. 561–569, Jan. 2018.

[37] H. Abbasi, M. Orouskhani, S. Asgari, and S. S. Zadeh, "Automatic brain ischemic stroke segmentation with deep learning: A review," *Neurosci. Informat.*, vol. 3, no. 4, Dec. 2023, Art. no. 100145.

[38] N. Niknejad, R. Bidese-Puhl, Y. Bao, K. G. Payn, and J. Zheng, "Phenotyping of architecture traits of loblolly pine trees using stereo machine vision and deep learning: Stem diameter, branch angle, and branch diameter," *Comput. Electron. Agricult.*, vol. 211, Aug. 2023, Art. no. 107999.

[39] K. Baratimehr, M. R. Moosavi, and H. Tahayori, "Measures for evaluating IT2FSs constructed from data intervals," *Appl. Soft Comput.*, vol. 136, Mar. 2023, Art. no. 110084.

[40] M. Alali, F. N. Shimim, Z. Shahooei, and M. Bahramipanah, "Intelligent line congestion prognosis in active distribution system using artificial neural network," in *Proc. IEEE Power Energy Soc. Innov. Smart Grid Technol. Conf. (ISGT)*, Feb. 2021, pp. 1–5.

[41] M. Farhang and F. Safi-Esfahani, "Recognizing MapReduce straggler tasks in big data infrastructures using artificial neural networks," *J. Grid Comput.*, vol. 18, no. 4, pp. 879–901, Dec. 2020.

[42] M. M. Saha, J. J. Izykowski, and E. Rosolowski, *Fault Location on Power Networks*. Berlin, Germany: Springer, 2009.

[43] K. Dubey and P. Jena, "Novel fault detection & classification index for active distribution network using differential components," *IEEE Trans. Ind. Appl.*, vol. 60, no. 3, pp. 4530–4540, May 2024.

[44] X. Dong, C. J. Taylor, and T. F. Cootes, "Defect classification and detection using a multitask deep one-class CNN," *IEEE Trans. Autom. Sci. Eng.*, vol. 19, no. 3, pp. 1719–1730, Jul. 2022.

[45] S. Jamali, A. Bahmanyar, and E. Bompard, "Fault location method for distribution networks using smart meters," *Measurement*, vol. 102, pp. 150–157, May 2017.

[46] R. H. Salim, K. C. O. Salim, and A. S. Bretas, "Further improvements on impedance-based fault location for power distribution systems," *IET Gener., Transmiss. Distrib.*, vol. 5, no. 4, p. 467, 2011.

[47] D. Thukaram, H. P. Khincha, and H. P. Vijaynarasimha, "Artificial neural network and support vector machine approach for locating faults in radial distribution systems," *IEEE Trans. Power Del.*, vol. 20, no. 2, pp. 710–721, Apr. 2005.

[48] S. Zare, M. S. Haghighi, M. R. Hairi Yazdi, A. Kalhor, and M. T. Masouleh, "Kinematic analysis of an under-constrained cable-driven robot using neural networks," in *Proc. 28th Iranian Conf. Electr. Eng. (ICEE)*, Iran, Aug. 2020, pp. 1–6.

[49] M. Tavasoli, M. H. Yaghmaee, and A. H. Mohajerzadeh, "Optimal placement of data aggregators in smart grid on hybrid wireless and wired communication," in *Proc. IEEE Smart Energy Grid Eng. (SEGE)*, Aug. 2016, pp. 332–336.

[50] H. Rezapour, S. Jamali, and A. Bahmanyar, "Review on artificial intelligence-based fault location methods in power distribution networks," *Energies*, vol. 16, no. 12, p. 4636, Jun. 2023.

[51] J. Fang, K. Chen, C. Liu, and J. He, "An explainable and robust method for fault classification and location on transmission lines," *IEEE Trans. Ind. Informat.*, vol. 19, no. 10, pp. 1–10, 2023.

[52] A. Keshavarz, R. Dashti, M. Deljoo, and H. R. Shaker, "Fault location in distribution networks based on SVM and impedance-based method using online databank generation," *Neural Comput. Appl.*, vol. 34, no. 3, pp. 2375–2391, Feb. 2022.

[53] F. Hariri and M. Crow, "New infeed correction methods for distance protection in distribution systems," *Energies*, vol. 14, no. 15, p. 4652, Jul. 2021.

[54] Y. Mousavi, G. Bevan, I. B. Kucukdemiral, and A. Fekih, "Active fault-tolerant fractional-order terminal sliding mode control for DFIG-based wind turbines subjected to sensor faults," in *Proc. IEEE IAS Global Conf. Emerg. Technol. (GlobConET)*, May 2022, pp. 587–592.

[55] Y. Mousavi, G. Bevan, I. B. Kucukdemiral, and A. Fekih, "Observer-based high-order sliding mode control of dfig-based wind energy conversion systems subjected to sensor faults," *IEEE Trans. Ind. Appl.*, vol. 60, no. 1, pp. 1750–1759, Feb. 2023.

[56] D. Tiwari, M. J. Zideh, V. Talreja, V. Verma, S. K. Solanki, and J. Solanki, "Power flow analysis using deep neural networks in three-phase unbalanced smart distribution grids," 2024, *arXiv:2401.07465*.

[57] S. S. Mohtavipour and M. J. Zideh, "An iterative method for detection of the collusive strategy in prisoner's dilemma game of electricity market," *IEEJ Trans. Electr. Electron. Eng.*, vol. 14, no. 2, pp. 252–260, Feb. 2019.

[58] M. Sarwar, F. Mehmood, M. Abid, A. Q. Khan, S. T. Gul, and A. S. Khan, "High impedance fault detection and isolation in power distribution networks using support vector machines," *J. King Saud Univ. Eng. Sci.*, vol. 32, no. 8, pp. 524–535, Dec. 2020.

[59] A. Ghaderi, H. A. Mohammadpour, H. L. Ginn, and Y.-J. Shin, "High-impedance fault detection in the distribution network using the time-frequency-based algorithm," *IEEE Trans. Power Del.*, vol. 30, no. 3, pp. 1260–1268, Jun. 2015.

[60] M. Tavasoli, E. Lee, Y. Mousavi, H. B. Pasandi, and A. Fekih, "WIPE: A novel web-based intelligent packaging evaluation via machine learning and association mining," *IEEE Access*, vol. 12, pp. 45936–45947, 2024.

[61] A. Sohani, H. Sayyaadi, and S. Hoseinpoori, "Modeling and multi-objective optimization of an M-cycle cross-flow indirect evaporative cooler using the GMDH type neural network," *Int. J. Refrigeration*, vol. 69, pp. 186–204, Sep. 2016.

[62] M. Tavasoli, *Web-Based Intelligent Packaging Evaluation (WIPE) Platform*. East Lansing, MI, USA: Michigan State University, 2023.

[63] M. M. Taleshi, N. Tajik, A. Mahmoudian, and M. Yekrangnia, "Prediction of pull-out behavior of timber glued-in glass fiber reinforced polymer and steel rods under various environmental conditions based on ANN and GEP models," *Case Stud. Construction Mater.*, vol. 20, Jul. 2024, Art. no. e02842.

[64] S. Awasthi, G. Singh, and N. Ahamad, "Classifying electrical faults in a distribution system using K-nearest neighbor (KNN) model in presence of multiple distributed generators," *J. Inst. Engineers (India), Ser. B*, vol. 105, no. 3, pp. 621–634, Jun. 2024.

[65] Z. Lin, D. Duan, Q. Yang, X. Hong, X. Cheng, L. Yang, and S. Cui, "Data-driven fault localization in distribution systems with distributed energy resources," *Energies*, vol. 13, no. 1, p. 275, Jan. 2020.

[66] M. Zhao and M. Barati, "A real-time fault localization in power distribution grid for wildfire detection through deep convolutional neural networks," *IEEE Trans. Ind. Appl.*, vol. 57, no. 4, pp. 4316–4326, Jul. 2021.

[67] S. Liu, H. Yin, Y. Zhang, X. Liu, and C. Li, "Fault location method for distribution network with distributed generation based on deep learning," in *Proc. 4th Int. Conf. Smart Power Internet Energy Syst. (SPIES)*, Dec. 2022, pp. 1157–1162.

[68] H. R. Baghaee, D. Mlakic, S. Nikolovski, and T. Dragicevic, "Support vector machine-based islanding and grid fault detection in active distribution networks," *IEEE J. Emerg. Sel. Topics Power Electron.*, vol. 8, no. 3, pp. 2385–2403, Sep. 2020.

[69] H. F. Eniser, S. Gerasimou, and A. Sen, "DeepFault: Fault localization for deep neural networks," in *Proc. Int. Conf. Fundam. Approaches Softw. Eng.* Switzerland: Springer, 2019, pp. 171–191.

[70] S. Jafari, S. Hoseinzadeh, and A. Sohani, "Deep Q-Value neural network (DQN) reinforcement learning for the techno-economic optimization of a solar-driven nanofluid-assisted desalination technology," *Water*, vol. 14, no. 14, p. 2254, Jul. 2022.

[71] S. Chakraborty, S. Das, T. Sidhu, and A. K. Siva, "Smart meters for enhancing protection and monitoring functions in emerging distribution systems," *Int. J. Electr. Power Energy Syst.*, vol. 127, May 2021, Art. no. 106626.

[72] K. Chen, J. Hu, Y. Zhang, Z. Yu, and J. He, "Fault location in power distribution systems via deep graph convolutional networks," *IEEE J. Sel. Areas Commun.*, vol. 38, no. 1, pp. 119–131, Jan. 2020.

ARASH MOUSAVI received the B.Sc. degree in control engineering from Payam University, Golpayegan, Iran, in 2013, and the M.Sc. degree in electrical engineering from Islamic Azad University, Iran, in 2016. He is currently a Lead Researcher with the Department of Electrical Engineering and Applied Sciences, Paradise Research Center, Jahrom, Iran. His research interests include data-driven techniques in power systems, artificial intelligence, power systems analysis, robust nonlinear control, distributed networks, and renewable energy.

RASHIN MOUSAVI received the B.Sc. degree in electrical engineering from Payam University, Golpayegan, Iran, in 2010. He is currently a Lead Researcher with the Department of Electrical Engineering and Applied Sciences, Paradise Research Center, Jahrom, Iran. His research interests include power systems analysis, data-driven techniques in power systems, artificial intelligence, linear and nonlinear control, distributed networks, and renewable energy.

YASHAR MOUSAVI (Member, IEEE) received the Ph.D. degree in control engineering from Glasgow Caledonian University, Glasgow, U.K., in 2023. He is currently a Senior Analytical Engineer with American Axle and Manufacturing, Detroit, Michigan, USA. He majored in artificial intelligence and machine learning-based modeling, simulation, and analysis of combustion-based and electric vehicles' driveline systems. He has carried out various projects for top-notch OEM companies, such as General Motors, Stellantis, Ford, Mercedes Benz, and Volkswagen. He is also a Controls Integration Researcher with the Power and Renewable Energy Systems (PRES) Team, Glasgow Caledonian University, Glasgow, U.K. His research interests include control theory and applications, machine learning, fault-tolerant control, renewable energy, wind turbines, vehicle dynamics modeling and analysis, artificial intelligence, power systems analysis, robust nonlinear control, and robotic systems modeling and control. He is a member of the IEEE Young Professionals. He has served as a reviewer and a guest editor for '

MAHSA TAVASOLI received the first M.Sc. degree in computer engineering from Ferdowsi University, Mashhad, Iran, in 2016, and the second M.Sc. degree in packaging from Michigan State University, MI, USA, in 2023. She is currently pursuing the Ph.D. degree in information technology with North Carolina Agricultural and Technical State University, USA, where she specializes in machine learning (ML) and digital twins (DT). Her research interests include applying ML and DT technologies to system implementations, communication network security, and privacy, with a particular focus on smart cities, including autonomous vehicles, smart healthcare, smart supply chains, and smart farming.

ALIASGHAR ARAB (Member, IEEE) received the B.S. degree in robotics engineering and the M.S. degree in electrical engineering from the Shahrood University of Technology, Iran, and the Ph.D. degree in mechanical and aerospace engineering from Rutgers University, New Brunswick, NJ, USA, in 2021. He was a Robotics Research Scientist with Nokia Bell Laboratories and Verizon Emerging Technology, NJ, USA. He is currently an Adjunct Professor with the NYU Tandon School of Engineering and the Director of the Agile Safe Autonomous Systems (ASAS) Laboratories. His research interests include nonlinear control, motion planning, nonlinear model predictive control, and safety-critical control systems. He is a member of the American Society of Mechanical Engineers (ASME) and the Association for the Advancement of Artificial Intelligence (AAAI).

AFEF FEKIH (Senior Member, IEEE) received the B.Sc., M.Sc., and Ph.D. degrees in electrical engineering from the National Engineering School of Tunis, Tunisia, in 1995, 1998, and 2002, respectively. She is currently a Full Professor with the Department of Electrical and Computer Engineering and the Chevron/BORSF Professor of engineering with the University of Louisiana at Lafayette. Her research interests include control theory and applications, including nonlinear and robust control, optimal control, and fault-tolerant control with applications to power systems, wind turbines, unmanned vehicles, and automotive engines. She is a member of the IEEE Control Systems Society, the IEEE Power and Energy Society, and the IEEE Women in Engineering Society. She is an Appointed Member of the Board of Governors of the IEEE Control Systems Society, from 2023 to 2024. She is also a member of the IFAC Technical Committee on Power and Energy Systems, the American Automatic Control Council (AACC) Technical Committee on Control Education, the IEEE Systems Council on Diversity and Inclusion Committee, and the IEEE Technology Conference Editorial Board. She is the Co-Chair and the Media Coordinator of the IEEE Control System Society Women in Control Group (WiC). She serves as an Associate Editor for the IEEE IAS, Industrial Automation and Control Committee. She has served as a reviewer and a guest editor for numerous journals and conferences.